# Proton Nuclear Magnetic Resonance Moment and Relaxation Study of Cellulose Morphology

**Alex. L. Mackay,*† Mark Tepfer,†§ Iain E. P. Taylor,‡ and Frank Volke‖**

*Departments of Physics and Botany, University of British Columbia, Vancouver, Canada, and Sektion Physik, Karl Marx Universitat, Leipzig, GDR.* *Received June 19, 1984*

ABSTRACT: Proton magnetic resonance ($^1$H NMR) has been used to determine the second moment ($M_2$) of the line shape, solid echo decay, and dipolar ($T_{1d}$), rotating frame ($T_{1\rho}$) and spin-lattice ($T_1$) relaxation times of unaltered, crystallite-enriched, and gelled-reprecipitated samples of cotton and filter paper cellulose. For all samples, the measured $M_2$ was within 30% of that for the rigid lattice, indicating that cellulose microfibrils are almost rigid on the $^1$H NMR time scale of $10^{-5}$ s. Measurements of $T_1$ as a function of frequency indicated the presence of a low amplitude but important motion occurring in cellulose at about 10–15 MHz which may be methylol group reorientation. Measurements of $T_{1d}$, $T_{1\rho}$, and the solid echo decay revealed the presence of two types of domains which we assign to crystalline and paracrystalline cellulose. Crystallite-enriched cellulose contained material of only one domain type. Cellulose of reduced crystallinity (gelled-reprecipitated) contained a corresponding increase in the domain we assigned to paracrystalline cellulose. Our results are in agreement with a model in which the crystalline cellulose domains consist of rigid crystalline microfibrils with cross-sectional widths of 100–400 Å and the paracrystalline cellulose domains consist of smaller elementary fibrils with lower packing density.

## Introduction

The elucidation of the structural and dynamic properties of cellulose is fundamental to understanding its role as a major constituent of the walls of plant cells. In native cellulose (cellulose I) the 1–4 linked $\beta$-D-glucose chains are oriented in parallel to form microfibrils.[1] Cellulose from natural sources contains both highly crystalline and paracrystalline (domains with some packing disorder) regions whose relative proportions depend upon the source and extraction procedure used.[2]

Nuclear magnetic resonance (NMR) techniques have provided information on both macromolecular structure and dynamics of cellulose.[3-10] In high-resolution, solid-phase $^{13}$C NMR studies of cellulose,[3-7] resolved lines have been observed from the C1, C4, and C6 carbons of the constituent glucose. The presence of inhomogeneous line broadening of the C4 and C6 lines has been attributed to packing disorder in paracrystalline regions and surface regions of the microfibrils. From a comparison of $^{13}$C NMR spectra of crystalline cellulose from several sources, Atalla and VanderHart[7] have recently proposed the existence of two different types of crystalline cellulose which they label $I_\alpha$ and $I_\beta$. The relative proportions of these two crystal structures were found to be different for cellulose from different biological sources.

Broad-line $^1$H NMR spectroscopic studies have also been carried out on cellulose.[8-10] In an earlier study,[10] we showed that almost all of the protons in cellulose microfibrils are essentially rigid on the proton NMR time scale of $10^{-5}$ s. The cellulose $^1$H NMR spectrum, which is determined by the dipolar interactions between neighboring protons, is broad and featureless and, consequently, not very sensitive to details of the crystal structure or to the degree of crystallinity of the cellulose microfibrils. $^1$H NMR relaxation measurements, on the other hand, are sensitive to subtle differences in molecular motions which are present in the different forms of cellulose. In this paper we report the use of several $^1$H NMR relaxation techniques to distinguish between the crystalline and paracrystalline domains of cellulose microfibrils.

†Department of Physics, University of British Columbia.
‡Department of Botany, University of British Columbia.
‖Sektion Physik, Karl Marx Universitat.
§Current address: Laboratoire de Biologie Cellulaire, I.N.R.A., 78000 Versailles, France.

## Materials

Three cellulose samples were used: cellulose I (99.3%) purified from cotton fiber (Hercules Inc., Wilmington, DE), Whatman No. 1 filter paper, and 100% cotton thread (J. P. Coates). Crystallite-enriched cellulose was prepared by the method of Ranby.[11] Cellulose of reduced crystallinity was obtained by treatment with 4-methylmorpholine *N*-oxide.[12] The gelled polymer was reprecipitated by rapid mixing with 10 volumes of water. All samples were extensively exchanged in $^2H_2O$ (99.8% $^2$H from Merck Sharpe and Dohme, Ltd) to minimize the water signal.[10]

## NMR Methods

Most of the $^1$H NMR results were acquired at room temperature (24 °C) on a Bruker SXP 4-100 pulse NMR spectrometer operating at 90 MHz. Total second moment, $M_2$, measurements were made from the NMR spectra.[10] Since the receiver recovery time at 90 MHz was about 8 $\mu$s, the free induction decays (FIDs) were extrapolated to the middle of the 90° pulse before Fourier transformation.[10] Some of the interpair second moments, $M_2'$ (interpair), were measured at 90 MHz on the UDRIS (Unical Doppel Resonz Impuls Spectrometer) spectrometer constructed by the group of Professor Pfiefer at the Sektion Physik, Karl Marx University, Leipzig, GDR.

For the dipolar relaxation measurements, the spectrometer was set on resonance and the Jeener echo pulse sequence,[13] $90_0$–$\tau_1$–$45_{90}$–$\tau_2$–$45_{90}$, was applied with $\tau_1$ fixed at 25 $\mu$s and with a series of values of $\tau_2$. The phase of the second pulse was alternated between 90° and 270° and the signal following the third pulse was alternately added and subtracted from the memory to minimize the contribution of the FID to the Jeener echo for short values of $\tau_2$ and to decrease the noise. For exponential dipolar relaxation

$$A_d(\tau_2,t) = A_d(0,t)\exp(-\tau_2/T_{1d}) \quad (1)$$

where $A_d(\tau_2,t)$ is the height of the Jeener echo at time $t$ following the third pulse. The quantity plotted against $\tau_2$ for $T_{1d}$ calculation was the mean echo height between $t$ = 10 and 15 $\mu$s. These two times span the echo maximum.

For the rotating frame relaxation measurements, the spectrometer was also set on resonance and the FID was recorded after the second pulse of a sequence consisting of a 90° pulse followed, after about 1 $\mu$s, by a long pulse shifted 90° in phase, of amplitude $H_1$ and of length $\tau$. For exponential rotating frame relaxation

$$A_\rho(\tau,t) = A_\rho(0,t)\exp(-\tau/T_{1\rho}) \quad (2)$$

0024-9297/85/2218-1124$01.50/0 

Table I
Measured Second Moment Values for the Cellulose Preparations[a]

| sample | | $10^{-9}M_2$, $s^{-1}$ |
|---|---|---|
| Whatman No. 1 filter paper | crystallite-enriched | 7.5 |
| | unaltered | 6.8 |
| | reprecipitated | 5.4 |
| Hercules chemical cotton | crystallite-enriched | 7.3 |
| | unaltered | 6.9 |
| | reprecipitated | 6.4 |
| J. P. Coates cotton thread | unaltered | 6.9 |

[a] The estimated experimental error is ±5%.

where $A_p(\tau,t)$ is the height of the FID at time $t$ following the second pulse. For this study, the behavior of $A_p(\tau,t)$ as a function of $\tau$ was investigated for three values of $\gamma H_1$ ($4.7 \times 10^4$, $1.9 \times 10^5$, and $3.5 \times 10^5$ $s^{-1}$) and two ranges of $t$, one between $t = 10$ and 15 μs and the second between $t = 92$ and 97 μs.

Spin–lattice relaxation measurements were made at eight Larmour frequencies: 90.0, 74.3, 51.3, 34.0, 25.0, 19.1, 15.2, and 11.2 MHz. For spin–lattice relaxation measurements at frequencies greater than 50 MHz, a 180° pulse was applied at a time, $\tau$, before every second 90° pulse and alternate scans were subtracted from the accumulative computer memory. For exponential relaxation

$$A(\tau,t) = A(0,t) \exp(-\tau/T_1) \quad (3)$$

where $A(\tau,t)$ is the FID intensity at time $t$ following the 90° pulse. For this study, $A(\tau,t)$ was measured for two values of $t$, one at about 14 μs and the other at about 300 μs.

For $T_1$ measurements at Larmor frequencies lower than 50 MHz, the receiver recovery time was sufficiently long to obscure most of the cellulose FID. For this situation, a third pulse, $90_{90}$, was applied at 15–30 μs after the second pulse and the signal amplitude, $A(\tau,t)$, was recorded at times ranging from 15 to 35 μs from the third pulse.

For all relaxation measurements, the time between transients, or sample recovery time, was 10 s ($\geq 5T_1$).

The measurement of the interpair second moment, $M_2'$(interpair), was derived from the variation with $\tau$ of the maximum amplitude of the solid echo following a $90_0$–$\tau$–$90_{90}$ pulse sequence. For a single $M_2'$(interpair) component, the echo maximum follows the relation

$$E(\tau) = E(0) \exp((-1/2)M_2'(\text{interpair})\tau^2) \quad (4)$$

To remove contributions to the echo from the residual FID due to protons with very small or zero average dipolar coupling, the signal following the sequence $90_0$–$\tau$–$180_{90}$ was subtracted from the solid echo signal.

## Results

All cellulose samples were prepared in excess $^2H_2O$, so the $^1H$ NMR signal arises from hydrogen sites which have not exchanged with the $^2H$ in the $^2H_2O$ or from the residual protons in the $^2H_2O$.

The FIDs from cellulose could be separated unambiguously into two components, a rapidly decaying fraction (decay constant $T_2^* \simeq 20$ μs) corresponding to nearly rigid protons and a slowly decaying fraction ($T_2^* \simeq 650$ μs) corresponding to much more mobile protons. The proportion of the FID from the rigid protons varied in different preparations, but was generally about 90% of the total FID.

The total second moment, $M_2$, was measured at 24 °C for cellulose from cotton fibers, cotton thread, Whatman No. 1 filter paper, crystallite-enriched cellulose from cotton and filter paper, and gelled–reprecipitated cellulose from cotton and filter paper. The $M_2$ for the more rigid component of the cellulose FID was obtained by dividing the measured $M_2$ by the fraction of the FID intensity in the rigid component,[10] i.e., the $M_2$ for the more mobile protons is assumed to be negligible. The second moment values are listed in Table I.

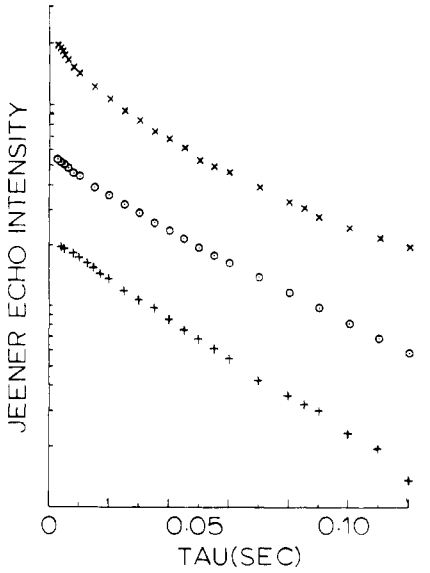


**Figure 1.** Dipolar relaxation of cellulose. The Jeener echo amplitude is plotted against $\tau_2$ for crystallite-enriched (+), unaltered (○), and reprecipitated (×) cotton fiber cellulose.

Table II
Dipolar Relaxation Times ($T_{1d}$) for the Cellulose Preparations[a]

| sample | | $T_{1d}$, ms | rel proportion, % |
|---|---|---|---|
| Whatman No. 1 filter paper | crystallite-enriched | 89 (88–89) | 100 |
| | unaltered | 48 (47–49) | 67 (58–73) |
| | | 4.3 (3.6–5.2) | 33 (27–42) |
| | reprecipitated | 11 (10.1–11.4) | 100 |
| Hercules chemical cotton | crystallite-enriched | 43 (43–44) | 100 |
| | unaltered | 56 (55–57) | 81 (80–82) |
| | | 8.4 (7.1–10) | 19 (18–20) |
| | reprecipitated | 60 (54–69) | 58 (50–64) |
| | | 9.8 (7.2–13) | 42 (36–50) |
| J. P. Coates cotton thread | unaltered | 55 (54–56) | 75 (74–76) |
| | | 7.7 (6.9–8.7) | 25 (24–26) |

[a] The ranges in parentheses represent the 68% probability limits for the relaxation times and proportions.

In Figure 1, the decay with $\tau_2$ of the Jeener echo amplitude is displayed for crystallite-enriched, unaltered, and gelled–reprecipitated filter paper cellulose. These types of curves, which, in most cases, cannot be accurately fitted to a single exponential, were found to be well represented by two exponentials. With a nonlinear functional minimization program,[14] the echo amplitudes and $\tau$ values were fitted to the sum of two exponentials, each of the form of eq 1. Points acquired at $\tau_2$ values less than 2 ms were neglected in the fit because of a nonnegligible contribution from the free induction decay in this region. The values obtained for the dipolar relaxation times, $T_{1d}$, of cellulose are listed in Table II.

We note that, although two components are found in the dipolar relaxation of cellulose, the shape of the Jeener echo

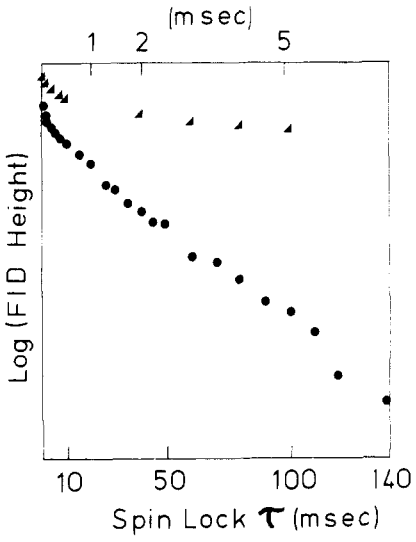


**Figure 2.** Rotating frame relaxation of unaltered cotton fiber cellulose. The FID amplitude (●) is plotted against the spin lock time, $\tau$, for $\gamma H_1 = 4.7 \times 10^4\ s^{-1} \simeq \gamma H_l$. The rapid decrease in amplitude (▲) at short $\tau$ values, shown in the expanded portion, is due to the initial equilibration of the magnetization along the spin-locking field.

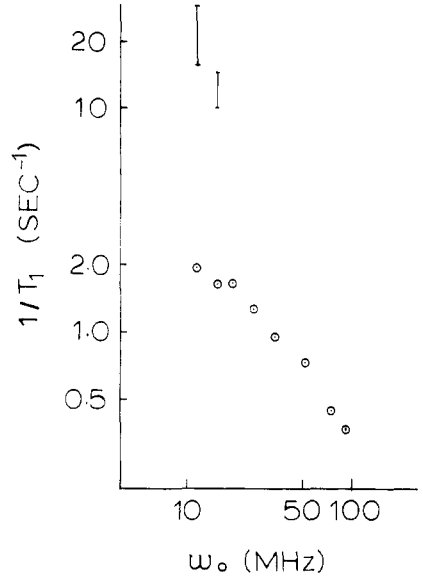


**Figure 3.** Spin–lattice relaxation of unaltered cotton fiber cellulose. $1/T_1$ is plotted as a function of the Larmor frequency on a log–log scale.

does not change substantially as either $\tau_1$ or $\tau_2$ is varied. This is an indication that the two components have similar $M_2$ values. The measurement of relative proportions of components with different dipolar relaxation rates by the Jeener echo technique is nontrivial. While a homogeneous sample has a Jeener echo intensity proportional to the derivative of the FID at time $\tau_1$, an inhomogeneous sample gives a superposition of such signals with relative intensities which, in general, depend upon $\tau_1$.

We proved that the relative intensities of components obtained from the Jeener echo measurements were meaningful by carrying out rotating frame relaxation measurements where such problems do not occur. The rotating frame relaxation behavior of cellulose (see Figure 2) is more complex than the dipolar relaxation behavior for two reasons. First, when the spin-locking field strength, $\gamma H_1$, is less than or of the same order as the proton dipolar field[15]

$$\gamma H_L' = (M_2/3)^{1/2} \tag{5}$$

there is, for times a few milliseconds after the pulse, an initial equilibration of the magnetization along the spin-locking field. Secondly, while the Jeener echo is generated only for protons with nonzero average dipolar interactions, the spin-locking experiment involves all protons in the sample; therefore, the rotating frame relaxation curve also contains a component from the mobile protons. Fortunately, both complications can be circumvented, the first by increasing the spin-locking pulse strength ($\gamma H_1 \gg \gamma H_L'$) and the second by selectively monitoring the decay of the rigid FID component. The cellulose $M_2$ of $6.9 \times 10^9\ s^{-2}$ corresponds to a proton local field, $\gamma H_L'$, of $4.8 \times 10^4\ s^{-1}$. We found that, for $\gamma H_1$ values of $4.7 \times 10^4$, $1.9 \times 10^5$, and $3.5 \times 10^5\ s^{-1}$, approximately 26%, 8%, and 0%, respectively, of the magnetization for unaltered cotton fiber cellulose was lost in the initial equilibration of the protons with the spin-locking field.

From the decay constants of the rotating frame relaxation curves, $T_{1\rho}$, one can derive the rotating frame relaxation time, $T_{1x}$, from the relation[16]

$$\frac{1}{T_{1\rho}} = \frac{1}{T_{1x}} \frac{H_1^2}{H_1^2 + H_L'^2} + \frac{1}{T_{1\rho}} \frac{H_L'^2}{H_1^2 + H_L'^2} \tag{6}$$

We found that, for $\gamma H_1 = 3.5 \times 10^5\ s^{-1}$, the unaltered cotton fiber cellulose had two $T_{1\rho}$ components with values of 47 ± 3 and 8 ± 3 ms with relative intensities of 82 ± 6% and 18 ± 6%, respectively. This corresponds to $T_{1x}$ values of 45 ± 3 and 8 ± 3 ms with the same relative proportions. It is important to note that the relative intensities of the $T_{1\rho}$ components were, within experimental error, equal to those for the dipolar relaxation components. Also, the rotating frame measurements gave no evidence for a component with $T_{1\rho} < 2$ ms; such a component could not have been detected in the dipolar relaxation measurements because of the presence of residual FID.

The rotating frame relaxation of the more mobile protons in the cotton fiber cellulose samples was found to be well represented by a single exponential corresponding to a $T_{1\rho}$ of about 100 ms.

In Figure 3, we show a plot of the spin–lattice relaxation times, $T_1$, for unaltered cotton fiber cellulose as a function of the Larmor frequency, $\omega_0$. For frequencies greater than or equal to 19 MHz, this relaxation was well described by a single exponential. The $T_1$'s of the more mobile and rigid protons in the cotton fiber sample differ only slightly in this range. This difference may be due to the presence of HDO on the surface of the sample. For Larmor frequencies less than 19 MHz, a second component in the relaxation curves was observed with $T_1 \leq 50$ ms. Because of the low signal-to-noise ratio and the fact that a solid echo sequence with $\tau = 30\ \mu s$ was employed, it is not practical to interpret quantitatively the nonexponential spin–lattice relaxation at lower $\omega_0$. However, at 15.2 MHz, the shorter component contributed about 10% to the total decay curve and, at 11.2 MHz, this component contributed about 30% of the decay curve intensity. In both cases, the echo intensity at the point where the data were recorded contained about a 55% contribution from the more rigid cellulose protons.

In Figure 4, the cotton fiber cellulose solid echo maximum is plotted as a function of the square of the time, $\tau$, between the two radio frequency pulses. Artifactual contributions to the echo peak intensity arising from the FID due to the more mobile protons in the sample have been eliminated by subtracting the signal following a $90_0$–$\tau$–$180_{90}$ pulse sequence. For the range of $\tau$ values used, there was no appreciable Hahn echo arising from this sequence.

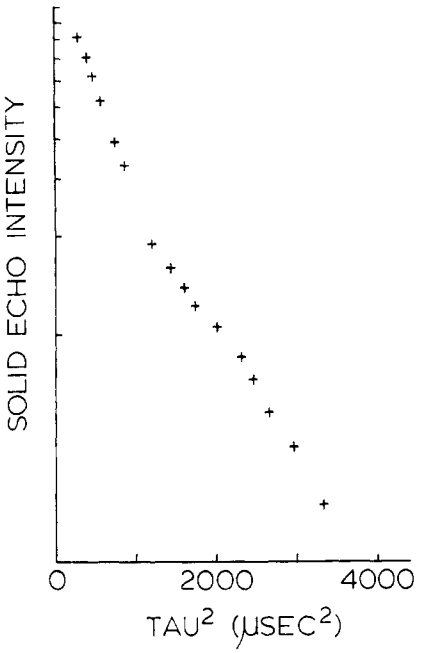


**Figure 4.** Spin pair dipolar echo decay of unaltered cotton fiber cellulose. The amplitude of the solid echo peak is plotted against the square of the time between the two 90° pulses.

**Table III**
**Interpair Second Moment Values for Cotton Fiber Cellulose[a]**

| sample | $10^{-9}M_2$(interpair), $s^{-2}$ | rel proportion, % |
|---|---|---|
| crystallite-enriched | 4.6 (4.4–5.0) | 88 (83–92) |
| | 1.1 (0.8–1.4) | 12 (8–17) |
| unaltered | 5.6 (5.2–6.1) | 77 (73–81) |
| | 1.6 (1.4–1.7) | 23 (19–27) |
| reprecipitated | 4.4 (3.4–5.9) | 67 (48–87) |
| | 1.5 (0.8–1.9) | 33 (13–52) |

[a] The values in parentheses represent the 68% probability limits for the moment values and proportions.

The solid echo decay curves for cotton fiber cellulose could not be well represented by a single Gaussian of the form of eq 4 but were relatively well fitted by nonlinear curve-fitting techniques[14] to the sum of two Gaussian components. Unfortunately this separation into two components was not so distinct as that for the dipolar relaxation data since (a) the two decay rates were not very different and (b) the smaller component had the longer decay rate. The values of $M_2'$(interpair) derived from the fits are related to the Van Vleck $M_2$(interpair) values (defined in the Discussion) by the factor 8/9.[17] The values of $M_2$(interpair) for each of the cotton fiber preparations are listed in Table III.

## Discussion

The results reported in this paper can be related to the microscopic structure of our cellulose preparations.

The most mobile component in our samples, which constitutes about 10% of the proton signal, is most likely from $^1H$ in the water and from "pockets" of $^1H_2O$ which have not exchanged with the added $^2H_2O$. Provided a large excess of water was present, the NMR properties of the rigid component of our samples were independent of the exact proportion of water. From this point, the discussion will relate to the more rigid component of the cellulose samples which makes up about 90% of the total proton intensity.

We can fit the dipolar relaxation curves for unaltered cellulose from cotton fibers and filter paper to two components, one with $T_{1d} \leq 10$ ms and 20–30% of the intensity and the other with $T_{1d} \simeq 50$ ms and 70–80% of the intensity. This indicates the presence of two separate populations of protons in the rigid components of our samples and the most likely assignment is to paracrystalline and crystalline domains. If cross-relaxation between the two domain types is negligible, this assignment would yield for our samples of filter paper, cotton thread, and cotton fiber paracrystalline contents of about 30%, 30%, and 20%, respectively, in approximate agreement with measurements on similar samples by other physical techniques.[2]

The proportions of crystalline and paracrystalline domains in cellulose can be altered by chemical means. The method of Ranby,[11] which involves preferential hydrolysis of surface or loosely packed regions of polymer, yields preparations with a high proportion of crystalline cellulose. The swelling of cellulose in 4-methylmorpholine *N*-oxide[12] loosens the polymer packing. Subsequent rapid immersion in water yields preparations with enhanced paracrystalline domains. When cellulose molecules recrystallize after swelling, it is probable that they have a cellulose II structure. Although the cellulose II crystal structure[18] is different from that of the naturally occurring celluose I, the broad-line $^1H$ NMR techniques which we use here to distinguish between crystalline and paracrystalline cellulose are not very sensitive to small differences in intermolecular separations on the level of the unit cell.

The interpretation that the two components of cellulose dipolar relaxation arise from crystalline and paracrystalline domains is strongly supported by the evidence (see Table II and Figure 1) that crystallite-enriched preparations of cotton and filter paper cellulose yielded only one $T_{1d}$ component—the one corresponding to the crystalline fraction—and that preparations of reprecipitated cellulose yielded a substantially increased fraction of the $T_{1d}$ component which corresponds to the paracrystalline fraction. Similar NMR relaxation behavior has also been observed for the amorphous and crystalline regions of several other polymer systems.[19–22]

There is considerable evidence from X-ray diffraction,[23,24] electron microscopy,[25] and computer modeling studies[18] that natural cellulose exists in the form of elementary fibrils with cross-sectional dimensions of 35 Å × 35 Å. These elementary fibrils aggregate in a regular manner to form larger crystalline microfibrils with sizes which depend upon the biological source of the cellulose. In cotton, microfibrils vary in cross-sectional width from 100 to 500 Å with an average width of about 250 Å.[24] We attribute the paracrystalline cellulose domains detected by proton NMR to regions of loosely packed elementary fibrils and the crystalline domains to regions where the fibrils are tightly aggregated into larger microfibrils.

Since they have different values of $T_{1d}$, the paracrystalline and crystalline fractions of cellulose must be present in separate domains. Since there should be dipolar contact at the domain boundaries, it is very important to determine whether cross-relaxation processes between domains have an appreciable effect on the dipolar relaxation results. If there was substantial cross-relaxation, the relative proportions of the two $T_{1d}$ components would not be equal to the relative amounts of paracrystalline and crystalline cellulose—in fact, the intensity of the faster decaying $T_{1d}$ component would represent a lower limit on the proportion of paracrystalline cellulose in the sample. Fortunately, the $M_2$ measurements provide us with an alternate means of estimating the relative amounts of crystalline and paracrystalline cellulose which is not susceptible to the effects of spin diffusion. For each sample we can represent the

experimental $M_2$ values in terms of the moments of the crystalline and paracrystalline fractions ($M_2$(cryst) and $M_2$(para), respectively) using

$$M_2(\text{exptl}) = f(\text{cryst})M_2(\text{cryst}) + f(\text{para})M_2(\text{para}) \quad (7)$$

where $f$(cryst) and $f$(para) (=1 − $f$(cryst)) refer to fractions of the two domain types. For $M_2$(cryst), we use the experimental $M_2$ values for the crystalline-enriched samples and for $M_2$(para) we use the experimental $M_2$ value for the gelled–reprecipitated filter paper sample. For these three samples the dipolar relaxation was single exponential. Using eq 7, we find that, for unaltered filter paper, $f$(cryst) = 0.67; for unaltered cotton fiber, $f$(cryst) = 0.79; and for gelled–reprecipitated cotton fiber, $f$(cryst) = 0.53. These numbers, which have an estimated error of 10–15%, are in excellent agreement with the corresponding fractions derived from $T_{1d}$ component intensities of 0.67, 0.81, and 0.58, respectively. Therefore, spin diffusion processes do not give rise to appreciable cross-relaxation during the dipolar relaxation time. In terms of cellulose morphology, this means that the crystalline microfibril must be sufficiently wide that the protons can retain dipolar polarization for times of order 50 ms, their $T_{1d}$ value, while the protons in the adjacent but more loosely packed fibrils relax to the lattice at a rate of order 10 ms. A lower limit for the cellulose microfibrillar cross-sectional width may be derived from the condition $L^2 > 4DT_{1d}$, where $D$, the spin diffusion constant for the migration of spin polarization in the crystalline domains, may be estimated from the relation[26]

$$D = a^2(M_2)^{1/2}/30 \quad (8)$$

where $a$ is the mean spacing between adjacent protons. For our cellulose samples we calculate a lower limit for the cross-sectional size of about 100 Å.

For a Larmor frequency of 19 MHz or greater, the cotton fiber cellulose was found to have a single $T_1$ value. The other cellulose samples had single-exponential spin–lattice relaxation at 90 MHz. Since they have different structures, one would expect paracrystalline and crystalline domains to have different $T_1$'s; indeed, such behavior has been observed for other polymers.[19] Therefore, we deduce that the cellulose microfibrillar cross-sectional widths are sufficiently small that spin diffusion processes are able to maintain a common spin temperature throughout the sample in a time shorter than $T_1$. This enables us to estimate an upper limit for cellulose microfibril widths. Using the above relations and the cellulose $T_1$ value of 0.6 s at 19 MHz, we obtain a value of about 400 Å for this upper limit. This is an important result because the microfibrillar cross section must be between 100 and 400 Å. This upper limit would be larger if the $T_1$ values for the different domains were close to the average value of 0.6 s, since then the sample could have a nearly uniform spin temperature in the absence of cross-relaxation. Measurements of cotton microfibril sizes by other techniques[24] have yielded widths between the limits derived above.

At this time we cannot deduce unambiguously the physical mechanisms for the $^1$H NMR relaxation processes in cellulose. One major difference between paracrystalline and crystalline domains which might account for the presence of two relaxation times in the dipolar and rotating frame measurements is the likely presence at the fibril surface of rotational disorder of the methylol group about the C5–C6 bond. If, in the limiting case, the dipolar relaxation times in paracrystalline and crystalline domains are completely determined by spin diffusion processes to the fibril surfaces, then the lower limit derived earlier for the microfibrillar sizes of 100 Å would represent the actual cross section and the paracrystalline $T_{1d}$ of about 8 ms would yield an estimated elementary fibril cross section of about 40 Å. It appears that a different process is responsible for spin–lattice relaxation at Larmor frequencies greater than 19 MHz, since the $T_1$ values are much longer. The behavior of $1/T_1$ as a function of the Larmor frequency cannot be fitted to a function of the form $\omega_0^{-2}$ which should obtain for a motion with a single correlation time and an exponential correlation function.[27] In fact, for cotton fiber cellulose, $1/T_1$ is approximately proportional to $\omega_0^{-0.8}$. Two approaches which have been used to characterize spin–lattice relaxation in polymers are defect diffusion models[19] and correlated-state models.[28] The correlated-state model, which employs a fractional exponential correlation function and has been shown to account for the temperature dependence of $T_1$, $T_{1\rho}$, $M_2$, and mechanical loss in a bulk polycarbonate,[28] seems to be capable of explaining the cellulose results. In this case the fundamental $T_1$ process would be torsional oscillations of the glucose monomers. The presence of more than one component in the spin–lattice relaxation decays at 15.2 and 11.2 MHz is presumably due to spatial inhomogeneities in the spectral density of fluctuations in the cellulose sample in this frequency range. For frequencies at or below 15 MHz the $T_1$ for some of the cellulose protons has changed by 1 order of magnitude from about 0.5 to about 0.05 s. This indicates the onset of an important motion of frequency about 15 MHz in the cellulose samples. Because, within experimental error, the shorter cotton cellulose $T_1$ at 11.2 MHz is equal to $T_{1d}$, it is likely that the two relaxation processes have the same mechanism. This implies that if the methylol group is indeed responsible, then its reorientations have a correlation time of order $10^{-7}$ s.

The spin pair dipolar echo experiment has been found useful for the measurement of the orientational order at proton sites for which one set of dipolar couplings is stronger than other dipolar couplings.[29,30] For this technique, it is convenient to separate the total Van Vleck second moment, $M_2$, into two parts, $M_2$(intrapair) and $M_2$(interpair), where for a solid powder

$$M_2 = \frac{9\gamma^4\hbar^2}{20N}\sum_{j=1,N}\sum_{k\neq j}\frac{1}{R_{jk}^6}$$

$$= \frac{9\gamma^4\hbar^2}{20N}\sum_{j=1,N}\frac{1}{R_{jl}^6} + \frac{9\gamma^4\hbar^2}{20N}\sum_{j=1,N}\sum_{k\neq j,l}\frac{1}{R_{jk}^6}$$

$$= M_2(\text{intrapair}) + M_2(\text{interpair}) \quad (9)$$

where $N$ is the total number of protons in the sample, $\gamma$ is the magnetogyric ratio for the proton, $\hbar$ is the Planck's constant divided by $2\pi$, $R_{jk}$ is the separation between protons $j$ and $k$, and proton $l$ is the proton closest to proton $j$.

For the unaltered cotton fiber cellulose sample we measure two Gaussian components in the solid echo decay which have an intensity distribution close to 80% and 20%—the proportions of cellulose with different $T_{1d}$'s. We therefore attribute these two cellulose components with $M_2$(interpair) of $(5.6 \pm 0.5) \times 10^9$ and $(1.6 \pm 0.3) \times 10^9$ s$^{-2}$ to crystalline and paracrystalline domains, respectively. As explained in the Results section, it was difficult to separate these two Gaussian components quantitatively. However, it is clear (see Table III) that the proportion of the component which we assign to crystalline domains is greater in the crystallite-enriched and smaller in the gelled–reprecipitated cellulose preparations. This type of

solid echo behavior has been observed for other polymers.[31]

With the use of eq 9 and the following assumptions concerning cellulose morphology, we have calculated values for $M_2$ and $M_2$(interpair) for crystalline and paracrystalline domains.

With the assumption that the crystalline microfibrils are absolutely rigid and undergo no hydrogen exchange with $^2H_2O$ the calculated $M_2$ value for crystalline cellulose is $7.3 \times 10^9$ s$^{-2}$, which is in very good agreement with the measured values for crystalline-enriched cotton fiber and filter paper of $7.5 \times 10^9$ and $7.3 \times 10^9$ s$^{-2}$. The calculated value of $M_2$(interpair) for this model of $4.2 \times 10^9$ s$^{-2}$ is, within experimental error, also consistent with the measured value of $(5 \pm 1) \times 10^9$ s$^{-2}$ for cotton fiber cellulose.

Since the elementary cellulose fibrils are relatively small, it has been assumed that all hydroxyl hydrogen sites are occupied by deuterons from the $^2H_2O$ and the intermolecular contribution to the second moment is reduced by half. It is assumed additionally that the C6 methylol groups on the fibril surface reorient rapidly (on the $^1$H NMR time scale of $10^{-5}$ s) about the C5–C6 axis. Evidence for the presence of motion or disorder of surface methylol groups in cellulose fibrils has been obtained from viscoelastic measurements,[32] dielectric measurements,[33] X-ray diffraction,[23] computer modeling,[18] and $^1$H NMR[33,34] and $^{13}$C NMR.[6] For an elementary fibril of cross section 35 Å $\times$ 35 Å, with 36 cellulose chains,[24] 39% of the methylol groups are distributed on the surface. The calculated $M_2$ for this model of paracrystalline cellulose is $5.4 \times 10^9$ s$^{-2}$. By combining the second moments of Table I with the relative proportions of $T_{1d}$ components in Table II we can derive an experimental $M_2$ value for paracrystalline cellulose using eq 7. The results are $M_2$(para) = $5.4 \times 10^9$ s$^{-2}$ for filter paper and $M_2$(para) = $5.2 \times 10^9$ s$^{-2}$ for cotton fiber, in excellent agreement with the above calculation. The calculated $M_2$(interpair) for this model of paracrystalline cellulose of $2.0 \times 10^9$ s$^{-2}$ is consistent with the measured value of $(1.5 \pm 0.5) \times 10^9$ within the experimental error.

## Concluding Remarks

On the basis of $^1$H NMR moments and relaxation times, we have been able to distinguish two fractions in cellulose I, which we ascribe to crystalline domains of microfibrils and paracrystalline domains of loosely packed elementary fibrils. It has been possible to put relatively narrow limits on the cross-sectional size of the microfibrils and to deduce the presence of rotational disorder in the methylol groups of the fibrils. These techniques can be applied to study the dynamics and structure of cellulose and other polysaccharides in plant cell walls.

**Acknowledgment.** We are grateful for the Natural Science and Engineering Research Council for financial support for this project. We thank Professor Myer Bloom and Edward Sternin for helpful discussions.

## References and Notes

(1) Gardner, K. H.; Blackwell, J. *Biopolymers* **1974**, *13*, 1975–2001.
(2) Wadsworth, L. C.; Cuculo, J. A. In "Modified Cellulosics"; Rowell, R. M., Young, R. A., Eds.; Academic Press: 1978; pp 117–46.
(3) Earl, W. L.; VanderHart, D. L. *Macromolecules* **1981**, *14*, 570–4.
(4) Maciel, G. E.; Kolodziejski, W. L.; Bertran, M. S.; Dale, B. E. *Macromolecules* **1982**, *15*, 686–7.
(5) Atalla, R. H.; Gast, J. C.; Sindorf, D. W.; Bartuska, V. J.; Maciel, G. E. *J. Am. Chem. Soc.* **1980**, *102*, 3249–51.
(6) Earl, W. L.; VanderHart, D. L. *J. Am. Chem. Soc.* **1980**, *102*, 3251–2.
(7) Atalla, R. H.; VanderHart, D. L. *Science* **1984**, *223*, 283–5.
(8) Harai, A.; Horii, F.; Kitamaru, R. J. *Polym. Sci.* **1980**, *18*, 1801–9.
(9) Forslind, E. *Nucl. Magn. Reson.* **1971**, *4*, 145–66.
(10) MacKay, A. L.; Bloom, M.; Tepfer, M.; Taylor, I. E. P. *Biopolymers* **1982**, *21*, 1521–34.
(11) Ranby, B. G. *Faraday Discuss. Chem. Soc.* **1981**, *11*, 158–64.
(12) Joseleau, J.-P.; Chambat, G.; Chumpitazi-Hermoza, B. *Carbohydr. Res.* **1981**, *90*, 339–44.
(13) Jeener, J.; Broekaert, P. *Phys. Rev.* **1967**, *157*, 232–40.
(14) James, F.; Roos, M. *Comput. Phys. Commun.* **1975**, *10*, 343–67.
(15) Goldman, M. "Spin Temperature and Nuclear Magnetic Resonance in Solids"; Oxford University Press: London, 1970; p 29.
(16) Reference 15, p 61.
(17) Boden, N.; Levine, Y. K. *J. Magn. Reson.* **1978**, *30*, 327–42.
(18) Sarko, A.; Muggli, R. *Macromolecules* **1974**, 486–94.
(19) Voigt, G.; Kimmich, R. *Polymer* **1980**, *21*, 1001–8.
(20) Bergmann, K. *Polym. Bull. (Berlin)* **1981**, *5*, 355–60.
(21) Ludwigs, K.; Geschke, D. *Ann. Phys. (Leipzig)* **1981**, *38*, 370–4.
(22) Packer, K.; Pope, J. M.; Yeung, R. R.; Cudby, M. E. A. *J. Polym. Sci., Polym. Phys. Ed.* **1984**, *22*, 589–616.
(23) French, A. D. *Carbohydr. Res.* **1978**, *61*, 67–80.
(24) Blackwell, J.; Kolpak, F. J. *Appl. Polym. Symp.* **1976**, *28*, 751–61.
(25) Ohad, I.; Danon, D. J. *Cell Biol.* **1964**, *22*, 302–4.
(26) Reference 15, p 65.
(27) Abragam, A. "The Principles of Nuclear Magnetism"; Oxford University Press: London, 1961; p 300.
(28) Jones, A. A.; O'Gara, J. F.; Inglefield, P. T.; Bendler, J. T.; Yee, A. F.; Ngai, K. N. *Macromolecules* **1983**, *16*, 658–65.
(29) Boden, N.; Mortimer, M. *Chem. Phys. Lett.* **1973**, *21*, 538–40.
(30) Volke, F.,; Arnold, K.; Gawrisch, K. *Chem. Phys. Lipids* **1982**, *31*, 179–89.
(31) Gotz, H.; Willing, T. *Plaste Kautsch.* **1982**, *11*, 661–3.
(32) Bradley, S. A.; Carr, S. H. *J. Polym. Sci., Polym. Phys. Ed.* **1976**, *14*, 111–24.
(33) Mikhailov, G. P.; Artyukov, A. I.; Shevelev, V. A. *Vysokomol. Soedin., Ser. A* **1969**, *A11*, 553–65.
(34) Nishinari, K.; Tsutsumi, A. *Macromolecules* **1984**, *22*, 95–9.